U.P.B. Sci. Bull., Series A, Vol. 81, Iss. 4, 2019 ISSN 1223-7027

BIFURCATIONS OF A HOLLING TYPE II COMMENSAL-HOST-PARASITE SYSTEM

Cristina Bercia[1]

The objective of this paper is to study the dynamical properties of the commensal-host-parasite differential system with 9 parameters, where the functional response of the parasite and the commensal species are of Holling type II. It is shown that the system has up to 8 equilibrium points, that saddle-node bifurcations occur or Hopf bifurcations from two different stationary solutions. From numerical simulations we found a situation of bistability for the system and we obtained phase portraits for different strata in the control parameter space induced by the topological equivalence. We detected two limit cycles in according with the analytical findings.

Keywords: Predator-prey system, Stability, Limit cycle, Bifurcation.

1. Introduction

Symbiotic relationships appear to be very common in biological and ecological communities [10]. There are generally identified three different symbiotic associations [9]. In mutualism, all the different species benefit from the interactions. In parasitism, the parasite get benefits at the expenses of the host, for instance bacteria, helmints and viruses fall generally in this category.

Commensalism denotes the interaction for which one organism benefits, but for the other one there is no gain or loss; for example golden jackals, who link themselves to a tiger maintaining a safe distance, feed on the remnants of the tiger's prey. Another example is the commensal microbiota that inhabit different parts of the gastrointestinal human tract and has been shaped by co-evolution with the host. The intestinal microbiota enhances resistence of the organism to infection by bacterial pathogens [5]. For example, the Lactobacillus bacteria alters the persistence of an gastrointestinal parasite (helminth) [8]. In ecology, in the commensal relation, the host organism is unmodified, whereas the commensal species may show great structural adaptation, for instance numerous birds perch on bodies of large mamal herbivores or feed on the insects turned up by grazing mammals.

Several scholars studied the dynamic behaviors of the commensalism or mutualism model for two species, for example in [1] a model with harvesting was proposed and in [11], a model with Allee efect, also [3] investigated a model with the equations of polynom-type.

In the present study, we consider three populations; commensal population $X(t)$, the host population $Y(t)$ and the parasite population $Z(t)$ at time t. The

---

[1] Lecturer, Faculty of Applied Sciences, University Politehnica of Bucharest, Romania, e-mail: `cristina_bercia@yahoo.co.uk`

model describing the interaction between them is governed by the following system of differential equations:

$$\begin{aligned} X'(t) &= r_1 X\left(1-\frac{X}{k_1}\right)+\frac{\alpha XY}{\alpha_1+Y}+\gamma XZ \\ Y'(t) &= r_2 Y\left(1-\frac{Y}{k_2}\right)-\frac{b_1 YZ}{\alpha_2+Y} \\ Z'(t) &= -mZ+\frac{b_2 YZ}{\alpha_2+Y}-\delta XZ \end{aligned} \tag{1}$$

In [2] it is a study of a close form of the model, but the term in the first equation $\frac{\alpha XY}{\alpha_1+Y}$ is replaced by $\frac{\alpha XY}{\alpha_1+X}$ and the dynamics appear not to contain any limit cycle which is a necessary condition for a realistic model [6].

The assumptions of the model include that the first and second population grow logistically, since both have sufficient resources for alternative foods. The parameters r_1, r_2 represent their intrinesc growth rate; k_1 is the environmental carrying capacity of the commensals, in the absence of all the other populations, the same is k_2 for the host population.

$\frac{\alpha Y}{\alpha_1+Y}$ represents the rate of consumption of one commensal per unit of time;

α_1 is the half saturation rate for the first population. Also it grows proportional with the parasite population, but there is no saturation effect when fedding upon the parasite. The host is not affected by the commensal and no recovery is possible for the host species once they get infected with the parasite.

$\frac{b_1 Y}{\alpha_2+Y}$ denotes the functional response of the parasite (i.e. the rate of consumption of one parasite); its form, known as Holling type II response function [6] is the same as the commensal's.

The third population has the rate m of mortality and grows only from interaction with Y, b_2 being the maximum growth rate of the parasite. The parameters are all strictly positive.

We adimensionalize the system, as follows:

$$tr_2=\tau; x(\tau)=\frac{X(t)}{k_1}; y(\tau)=\frac{Y(t)}{k_2}; z(\tau)=\frac{Z(t)}{k_2}; \frac{r_1}{r_2}=r; \frac{\alpha}{r_2}=a; \frac{\gamma k_2}{r_2}=b; \tag{2}$$

$$\frac{\alpha_1}{k_2}=c; \frac{\alpha_2}{k_2}=d; \frac{\delta k_1}{r_2}=\theta; \frac{b_1}{r_2}=\beta_1; \frac{b_2}{r_2}=\beta_2; \frac{m}{r_2}=\mu$$

We keep the notation $x'=\frac{dx}{d\tau}$ and the system (1) becomes:

$$\begin{aligned} x' &= rx(1-x)+\frac{axy}{c+y}+bxz \\ y' &= y(1-y)-\frac{\beta_1 yz}{d+y} \\ z' &= -\mu z+\frac{\beta_2 yz}{d+y}-\theta xz \end{aligned} \tag{3}$$

We consider the biologically meaningful initial conditions $x(0), y(0), z(0) \geq 0$.

Proposition 1.1. *The domain $\mathbb{R}^3_+$ is an invariant set of the system (3).*

Proof. If (v_1, v_2, v_3) is the vector-field which defines the differential system (3), $v_1\,|_{x=0}\,=0$, therefore all trajectories which initiate in this plane, remain in it,

$\forall t \geq 0$, so the plane $x = 0$ is an invariant set for the system. Similar arguments, $v_2\,|_{y=0} = 0$ and $v_3\,|_{z=0} = 0$ imply that $y = 0$ and $z = 0$ are also invariant sets and the three coordinate planes separate the interior of the first octant, which also will be invariant under the flow generated by the system. ☐

Proposition 1.2. *Every solution of the system (3) with positive initial values, is bounded.*

Proof. Let $(x(t), y(t), z(t))$ be such a solution. We know from the previous proposition that its components remain positive for any future time.

Denote by $U(t) = \frac{\theta}{b}x(t) + \frac{\beta_2}{\beta_1}y(t) + z(t)$. Then $U'(t) < \frac{r\theta}{b}x(1-x) + \frac{a\theta}{b}x + \frac{\beta_2}{\beta_1}y(1-y) - \mu z \leq \frac{(r+a)\theta}{b}(\frac{r+a}{r} - x) + \frac{\beta_2}{\beta_1}(1-y) - \mu z$.
So, $U'(t) < C - \frac{(r+a)\theta}{b}x(t) - \frac{\beta_2}{\beta_1}y(t) - \mu z(t)$, $\forall t \geq 0$, where $C = \frac{(r+a)^2\theta}{br} + \frac{\beta_2}{\beta_1} > 0$.
If $M = \min(1, r+a, \mu)$, then $U'(t) < C - MU(t)$, $\forall t \geq 0$. We obtain
$U(t) \leq (U(0) - \frac{C}{M})\exp(-Mt) + \frac{C}{M}$, that is $U(t) \leq \max(U(0), \frac{C}{M})$, $\forall t \geq 0$ and $U(t)$ is bounded. Since the first octant is an invariant set, the solutions starting in it are bounded. ☐

2. The equilibrium points and their stability

We determine the location of the equilibrium points of the system (3) and we state criteria that guarantee their existence. For any values of the parameters, the system admits the trivial equilibrium $E_0(0,0,0)$, the axial equilibria $E_1(1,0,0), E_2(0,1,0)$ and the parasite-free equilibrium $E_3(x_3, 1, 0)$, where
$x_3 = \frac{a}{r(c+1)} + 1$. There exists a commensal-free point of equilibrium $E_4(0, y_4, z_4)$, where $y_4 = \frac{d\mu}{\beta_2 - \mu}$, $z_4 = \frac{\beta_2 d[\beta_2 - \mu(1+d)]}{\beta_1(\beta_2-\mu)^2}$, iff $\beta_2 > \mu(1+d)$. The system has an interior equilibrium $E_5(x_5, y_5, z_5)$ with $x_5, y_5, z_5 > 0$, where $x_5 = (\frac{\beta_2 y_5}{d+y_5} - \mu)\frac{1}{\theta}$, $z_5 = \frac{(1-y_5)(d+y_5)}{\beta_1}$, iff $y_5 \in (0,1)$ is a solution of the equation:

$$f(y) \overset{\text{def}}{=} \frac{r}{\theta}\frac{[\beta_2 y - (\theta+\mu)(y+d)]}{d+y} - \frac{ay}{c+y} - \frac{b}{\beta_1}(1-y)(d+y) = 0 \tag{4}$$

with necessary conditions that $y_5 > \frac{d(\mu+\theta)}{\beta_2-\mu-\theta}$ and $\beta_2 > (d+1)(\mu+\theta)$.

Proposition 2.1. *Let*

$$d > \frac{a\theta\beta_1 c}{(c+1)((\theta+\mu)\beta_1 r + 2bc\theta) + a\theta\beta_1} \overset{\text{def}}{=} d_0. \tag{5}$$

If there is an interior equilibrium E_5*, then*

$$\beta_2 > (d+1)(\theta + \mu + \frac{a\theta}{r(c+1)}) \overset{\text{def}}{=} \beta_2^2. \tag{6}$$

Proof. The equation (4) can be written in the form

$$\beta_2 = h(y) \overset{\text{def}}{=} \frac{d+y}{y}[\theta + \mu + \frac{a\theta y}{r(c+y)} + \frac{b\theta}{r\beta_1}(1-y)(d+y)], y \in (0,1) \tag{7}$$

and $h(1) = \beta_2^2$. Simple calculations give us that
$h(y) - h(1) = \frac{d(\theta+\mu)(1-y)}{y} + \frac{a\theta(d-c)(1-y)}{r(c+1)(c+y)} + \frac{b\theta}{r\beta_1}\frac{(1-y)(d+y)^2}{y}$. If d is not too small, i.e. it is at least a fraction of c and verifies (5), then $h(y) > h(1)$. ☐

Proposition 2.2. *If $\beta_2 > \beta_2^2$, the system has one, two or three interior equili-bria. The second case happens if there exists $y \in (0,1)$ such that $\beta_2 = h(y)$ and $h'(y) = 0$. For the values $\{\beta_2 | \beta_2 = h(y), h'(y) > 0\}$, there are three interior equilibria. For all other values of β_2, there exists only one interior equilibrium.*

Proof. Denote by $f(y, \beta_2) = 0$ the equation (4), defined for $y \in (A \overset{\text{def}}{=} \frac{d(\mu+\theta)}{\beta_2-\mu-\theta}, 1)$. The condition $\beta_2 > \beta_2^2$ gets the form $f(1, \beta_2) > 0$. Note also that $f(A, \beta_2) < 0$. Since the equation in y is equivalent to a fourth order equation, it implies that on the interval $(A, 1)$ it has 1,2 or 3 distinct solutions. The second case is when one solution is double, one is distinct and it occurs if there exists y such that
$\{f(y, \beta_2) = 0, \frac{\partial f}{\partial y} = 0\} \Leftrightarrow \{\beta_2 = h(y), h'(y) = 0\}$.
Also, we have $\beta_2 - h(y) = \frac{\theta(d+y)}{ry} f(y, \beta_2)$, so the set $\{\beta_2 | \beta_2 = h(y), h'(y) > 0\}$= $\{\beta_2 | f(y, \beta_2) = 0, \frac{\partial f}{\partial y} < 0\}$. Then, due to the signs of f for y in A and 1, we obtain for these values of β_2, the case when there are three interior equilibria. (The numerical simulations illustrate these conclusions, see fig. 5) □

Using propositions (2.1) and (2.2), we get the following result:

Theorem 2.1. *1) If $\beta_2 < \mu(1 + d) \overset{\text{def}}{=} \beta_2^0$, the system (3) has four equilibria E_0, E_1, E_2, E_3.*
2) If $\beta_2^0 < \beta_2 < \beta_2^2$, there exist E_0, E_1, E_2, E_3 and E_4. If $d > d_0$, there is no interior equilibrium.
3) For $\beta_2 > \beta_2^2$, the system has the equilibria E_i, $i = \overline{0, 4}$ and generically, a single interior equilibrium or three.

We are now discussing the local stability of the equilibria. The Jacobian matrix J of the system, evaluated at each equilibrium gives explicit eigenvalues for the boundary equilibria, as follows: $J(E_0)$ has $\lambda_1 = r, \lambda_2 = 1, \lambda_3 = -\mu$;
$J(E_1)$ has $\lambda_1 = -r, \lambda_2 = 1, \lambda_3 = -\mu - \theta$;
For $J(E_2)$, $\lambda_1 = r + \frac{a}{c+1}, \lambda_2 = -1, \lambda_3 = -\mu + \frac{\beta_2}{d+1}$;
$J(E_3)$ has $\lambda_1 = -r - \frac{a}{c+1}, \lambda_2 = -1,\ \lambda_3 = \frac{\beta_2}{d+1} - (\mu + \theta + \frac{a\theta}{r(c+1)})$;

For $J(E_4)$, $\lambda_1 = r + \frac{ad\mu}{c(\beta_2-\mu)+d\mu} + bz_4$, and $\lambda_{2,3}$ verify the equation
$\lambda^2 + \frac{\mu[\beta_2(d-1)+\mu(1+d)]}{\beta_2(\beta_2-\mu)}\lambda + \mu[1 - \frac{\mu(1+d)}{\beta_2}] = 0.$

If $d < 1$ and $\beta_2 > \frac{\mu(1+d)}{1-d} \overset{\text{def}}{=} \beta_2^1$, we find that $Re(\lambda_{2,3}) > 0$.
If $d > 1$ or $\beta_2 \in (\mu(1 + d), \beta_2^1)$, it implies $Re(\lambda_{2,3}) < 0$.

Remark 2.1. *i) $\beta_2^1 < \beta_2^2$ is equivalent with $d < \frac{\theta[a+r(c+1)]}{\theta a+(\theta+\mu)r(c+1)} \overset{\text{def}}{=} d_1$.*
ii) Let be $d < 1$. For any combination of the other parameters, $\beta_2^0 < min(\beta_2^1, \beta_2^2)$.

We also compute the eigenvectors of $J(E_i)$ for $i = \overline{0, 4}$, to determine the liniar eigenspaces tangents to the stable or unstable manifolds of the equilibria. If we recall that the planes $x = 0$, $y = 0$, $z = 0$ are invariant sets for the system, we can find the stable manifolds for E_i.

Theorem 2.2. *1) The equilibrium point E_0 is a saddle, for any values of the parameters, attractive in the Oz-direction, repulsive in the directions of Ox and Oy;*
2) E_1 is always a saddle, with xOz the stable manifold;

3) E_2 *is always a saddle, attractive in the* Oy *direction, repulsive in* Ox *direction;*
4) If $\beta_2 < \beta_2^0$*, then* E_3 *is a stable node;*
5) Let $d < 1$*. If* $\beta_2 \in (\beta_2^0, \beta_2^1)$*, for* $d < d_1$ *or if* $\beta_2 \in (\beta_2^0, \beta_2^2)$*, for* $d > d_1$*, then* E_3 *is a stable node and* E_4 *is a saddle, with* yOz *the stable manifold;*
6) Let $d < d_1$*. If* $\beta_2 \in (\beta_2^1, \beta_2^2)$*, then* E_4 *is an unstable focus (or node) and* E_3 *is a stable node. If* $\beta_2 > \beta_2^2$*, only* E_3 *changes its stability into a saddle with* xOy *the stable manifold;*
7) Let $d < 1$*. If* $\beta_2 \in (\beta_2^2, \beta_2^1)$*, for* $d > d_1$*, then* E_3 *and* E_4 *are saddles. If* $\beta_2 > \beta_2^1$*, only* E_4 *changes its stability into an unstable focus (node);*
8) Let $d \geq 1$*. If* $\beta_2 > \beta_2^0$*,* E_4 *is a saddle. If* $\beta_2 \in (\beta_2^0, \beta_2^2)$*,* E_3 *is a stable node and for* $\beta_2 > \beta_2^2$*,* E_3 *is a saddle.*

Next we consider the dynamics of the system in the neighborhood of an interior equilibrium E_5. The linear part of the system at this equilibrium is determined by the Jacobian matrix $J(E_5) = (a_{ij})_{1\leq i,j\leq 3}$,

$$a_{11} = -\left(\frac{\beta_2 y_5}{d+y_5} - \mu\right)\frac{r}{\theta}; a_{12} = -\frac{ac}{(c+y_5)^2}\frac{a_{11}}{r}; a_{13} = \frac{b}{r}a_{11}; \tag{8}$$
$$a_{22} = \frac{y_5(1-d-2y_5)}{d+y_5}; a_{23} = -\frac{\beta_1 y_5}{d+y_5}; a_{31} = -\frac{\theta(1-y_5)(d+y_5)}{\beta_1};$$
$$a_{32} = \frac{d\beta_2(1-y_5)}{\beta_1(d+y_5)}; a_{21} = a_{33} = 0$$

where y_5 verifies the equation (4).

The eigenvalues of $J(E_5)$ are the solutions of the characteristic equation

$$\lambda^3 + A_1\lambda^2 + A_2\lambda + A_3 = 0, \tag{9}$$

where

$$A_1 = -a_{11} - a_{22}, A_2 = a_{11}a_{22} - a_{13}a_{31} - a_{23}a_{32}$$

and

$$A_3 = a_{22}a_{13}a_{31} + a_{11}a_{23}a_{32} - a_{12}a_{23}a_{31}.$$

Using the Routh-Hurwitz criterion, E_5 is asymptotically stable iff $A_1A_2 > A_3$, $A_1 > 0$ and $A_3 > 0$. The first two inequalities are satisfied if $y_5 > \frac{1-d}{2}$ or equivalent, $a_{22} < 0$.

$$A_1A_2 - A_3 = a_{11}a_{13}a_{31} + a_{22}a_{23}a_{32} + a_{12}a_{23}a_{31} - a_{11}a_{22}(a_{11} + a_{22}) \tag{10}$$

Note also that $A_3 > 0$ iff the condition $f'(y_5) > 0$ holds, or equivalently $h'(y_5) < 0$, where f and h are given by (4) and (7), respectivelly. So we proved the following result:

Theorem 2.3. *If the system (3) admits an interior equilibrium (for* $d > d_0$*, the condition is* $\beta_2 > \beta_2^2$*), then* $E_5(x_5, y_5, z_5)$ *is locally asymptotically stable iff* $A_1 > 0$*,* $h'(y_5) < 0$ *and* $A_1A_2 - A_3$ *given by (10) is strictly positive. A suficient condition for its local attractivity is* $y_5 > \frac{1-d}{2}$ *and* $h'(y_5) < 0$*.*

3. The bifurcation analysis

We consider β_2, the maximum growth rate of the parasite as a control parameter. First, we determine its values for static bifurcation, i.e. when β_2 passes through these values, the number of equilibria and their stability properties change. In $\mathbb{R}^3_+ \times \{\beta_2 > 0\}$, the branches of equilibria E_2 and E_4 intersect for $\beta_2 = \beta_2^0 = (d+1)\mu$. For $\beta_2 < \beta_2^0$, E_2 has $xOy = W^s$ the stable manifold and for $\beta_2 > \beta_2^0$, W^s is of dimension 1. So in $\beta_2 = \beta_2^0$ there is a change of stability and this is a static bifurcation. For $\beta_2 = \beta_2^2$, the branches of the boundary equilibrium E_3 and the interior equilibrium E_5 intersect. E_3 changes from a stable node for $\beta_2 < \beta_2^2$, into a saddle with $dimW^s = 2$ for $\beta_2 > \beta_2^2$, where as E_5 is physical only for $\beta_2 > \beta_2^2$. We find the second point of static bifurcation.

We return to the characteristic equation for an interior equilibrium (9).

Theorem 3.1. *If there exist* $y \in (0,1)$ *and* $\beta_2 > \beta_2^2$ *such that*

$$\begin{gathered} \beta_2 = h(y), \\ h'(y) = 0, \quad A_1, A_2 \neq 0, \end{gathered} \tag{11}$$

then for these values of β_2*, saddle-node bifurcations take place. If* (E_5, β_2^3) *is such a point in* $\mathbb{R}^3_+ \times \{\beta_2 > 0\}$ *with* $y_5 = y$*, the branches of the interior equilibria in the vicinity of this point remain on one side of* $\beta_2 = \beta_2^3$*, and no interior equilibria on the other side. (see fig. 5 with the bifurcation diagram for a numerical simulation)*

Proof. An interior equilibrium E_5 has its second coordinate y_5 which verifies equation (4) or equivalently (7), $\beta_2 = h(y_5)$. If $h'(y_5) = 0$, we saw in the proposition (2.2) that $\beta_2 = h(y)$ has a double solution and one, distinct. On the other hand, $h'(y_5) = 0 \Longleftrightarrow A_3 = 0$ from the characteristic equation, hence the jacobian matrix evaluated at E_5 has one eigenvalue, $\lambda_1 = 0$. Since $A_1, A_2 \neq 0$, there is no other eigenvalue with zero real part. Let (y_5, β_2^3) be a solution of the system (11). We write the system (3) in the form $v' = F(v, \beta_2)$, $v = (x, y, z)$. The matrix

$$\left(\frac{DF}{Dv} \,\middle|\, \frac{\partial F}{\partial \beta_2} \right)\Bigg|_{(E_5, \beta_2^3)} = \begin{pmatrix} a_{11} & a_{12} & a_{13} & 0 \\ 0 & a_{22} & a_{23} & 0 \\ a_{31} & a_{32} & 0 & \frac{y_5(1-y_5)}{\beta_1} \end{pmatrix} \tag{12}$$

has the rank 3 because $a_{11} \neq 0$, since $y_5 > \frac{d\mu}{\beta_2 - \mu}$.
Hence $rank\left(\frac{DF}{Dv} | \frac{\partial F}{\partial \beta_2}\right)$ for E_5 at the critical parameter value, is different from the rank of the Jacobian matrix. This is the nondegeneracy condition for the saddle-node bifurcation.(see [7], pg.71) ☐

We investigate also the bifurcation from an equilibrium of a limit cycle, i.e. the appearance of a periodic solution. Only the equilibria E_4 and E_5 may experience Hopf bifurcation, because these are the equilibrium points that can have a pair of purely imaginary eigenvalues.

Let us consider again the characteristic equation for an interior equilibrium $E_5(x_5, y_5, z_5)$ and its coefficients given by (9),(10).

Theorem 3.2. *The point* (E_5, β_2^H) *is a Hopf bifurcation point for an interior equilibrium iff the pair* $(y_5, \beta_2 = \beta_2^H)$ *verifies the system*

$$A_1 A_2 - A_3 = 0; \quad \beta_2^H = h(y_5) \tag{13}$$

together with the conditions

$$\frac{b(d+y_5)^2}{\beta_1 y_5} + \frac{d\beta_2^H}{y_5(\beta_2^H-\mu)-d\mu} > \frac{r(1-d-2y_5)}{\theta(1-y_5)} \tag{14}$$

$$\frac{\partial}{\partial\beta_2}[A_1A_2-A_3]\Big|_{\beta_2=\beta_2^H} \neq 0 \tag{15}$$

$$s \overset{\text{def}}{=} \beta_2^H - \frac{\theta(1-y_5)}{r} + \frac{(d+y_5)(r\mu-\theta y_5)}{ry_5} \neq 0 \tag{16}$$

The bifurcation takes place on a 2-dimensional manifold, namely the center manifold. If $s>0$, the manifold is attracting and if $s<0$, the center manifold is repelling. If $d>d_0$, then $\beta_2^H > \beta_2^2$.

Proof. The characteristic equation (9) for an interior equilibrium E_5 has the roots $\lambda_{1,2} = \pm i\omega$ iff $A_1A_2 = A_3$ and $A_2 > 0$. The inequality takes the form (14).
Suppose $\lambda_{1,2}(\beta_2) = \nu(\beta_2) \pm i\omega(\beta_2)$ is the analytic continuation of the imaginary eigenvalues near the critical parameter value $\beta_2 = \beta_2^H$.
The nondegeneracy condition for Hopf bifurcation is $\lambda_3(\beta_2^H) \neq 0$. We get $\lambda_3(\beta_2^H) = -A_1$ and $sgn(s) = sgn(A_1)$, so the condition is written in the form (16). For the transversality condition $\nu'(\beta_2^H) \neq 0$, simple algebra gives that $\nu(\beta_2)$ verifies the equation

$$8\nu^3 + 8\nu^2 A_1 + 2(A_2 + A_1^2)\nu + A_1A_2 - A_3 = 0$$

on a small neighborhood of $\beta_2 = \beta_2^H$. We obtain

$$\nu'(\beta_2^H) = \frac{\partial}{\partial\beta_2}[A_3 - A_1A_2]\frac{1}{2(A_2+A_1^2)}\Big|_{\beta_2^H},$$

so the transversality condition is equivalent to (15). From [4] theorems 5.2 and 5.4, we deduce that there exists a parameter dependent, local 2-dimensional invariant manifold (the center manifold) where a limit cycle bifurcates from the interior equilibrium, for β_2 near β_2^H. Due to the sign of λ_3 at β_2^H, the manifold is attracting for the system, iff $s > 0$. ☐

The direction and type of bifurcation will be investigated with numerical methods.

Remark 3.1. *If $d<1$, the pair $\left(E_4, \beta_2^1\right)$ is also a Hopf bifurcation point because the characteristic polynomial for E_4 has $\lambda_{2,3} = \pm i\omega$ iff $\beta_2 = \frac{\mu(1+d)}{1-d} \overset{\text{def}}{=} \beta_2^1$ and $d<1$.*

For β_2 in a neighborhood of β_2^1, let the analytic continuation of the pair of imaginary eigenvalues be $\lambda_{2,3}(\beta_2) = \nu(\beta_2) \pm i\omega(\beta_2)$. The transversality condition is $\nu'(\beta_2^1) \neq 0$ and we get $\nu'(\beta_2^1) = \frac{1}{2}(\lambda_2+\lambda_3)'(\beta_2^1) = \frac{(1-d)^3}{8\mu d} > 0$.
Note that $\lambda_1 > 0$ at the critical parameter value, so the central manifold where the bifurcation takes place is repelling for the system. Numerical simulations in the next section will show that this manifold where the bifurcation takes place is the plane $x = 0$.

4. **Numerical simulations**

We considered β_2 as a control parameter.

First, the fixed parameters are $a = 0.6; b = 0.8; c = 0.5; d = 0.1; \mu = 0.2; \theta = 0.4; \beta_1 = 0.3; r = 2$. It verifies $d > d_0 = 0.0329$ and $d < d_1 = 0.7058$.

We plot the curve $\beta_2 = h(y)$ given by (7) for $y \in (0, 1)$ and we find that for each value of β_2, the equation has only one solution (proposition 2.2, when h is strictly decreasing on $(0, 1)$). The values of β_2 when the topological structure of the phase portrait changes are the static bifurcation values $\beta_2^0 = 0.22; \beta_2^2 = 0.748$ and we found also Hopf bifurcation point for the equilibrium E_4 at the critical parameter value $\beta_2^1 = 0.244$. For the interior equilibrium E_5, we applied theorem 3.2. We solved numerically the system (13) which gives the pair $(y_5, \beta_2^H) = (0.34104; 1.0393)$ and the nondegeneracy and the transversality conditions are verified.

Then we represented the phase portrait for each stratum in the control parameter's space to illustrate our theoretical findings.

For $\beta_2 \in (\beta_2^0, \beta_2^1)$, we took $\beta_2 = 0.23$ and with a programe in MATLAB, we obtained representative orbits.

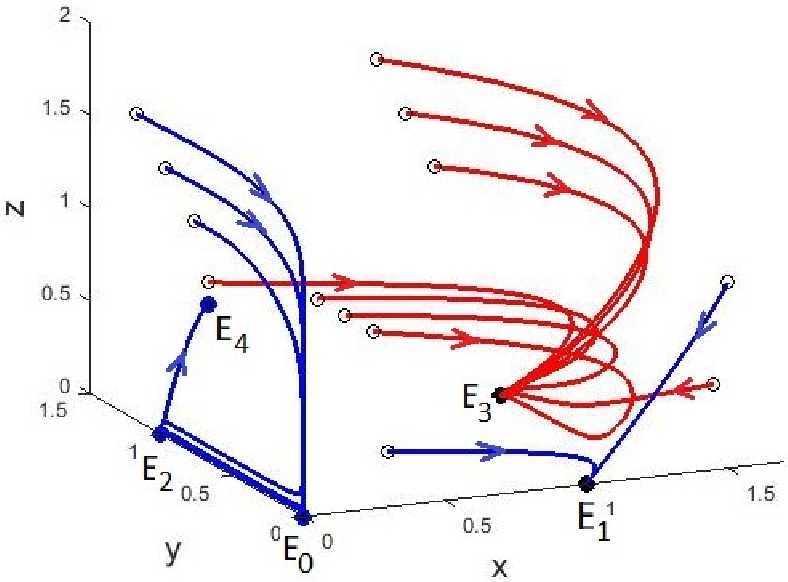

Figure 1. The phase portrait for $a = 0.6; b = 0.8; c = 0.5; d = 0.1; \mu = 0.2; \theta = 0.4; \beta_1 = 0.3; r = 2$. The control parameter is $\beta_2 = 0.23 \in (\beta_2^0, \beta_2^1)$. There is no interior equilibrium. The equilibrium $E_3(1.2; 1; 0)$ is globally asymptotically stable for $(\mathbb{R}_+^*)^3$ where the red orbits initiate. $E_1(1, 0, 0)$ has $y = 0$ its stable manifold. $E_4(0; 0.6666; 0.8518)$ captures for $t \to \infty$ all trajectories from the plane $x = 0$.

More than the statement of the theorem 2.2, 5), the numerical simulations which we performed, lead to the idea that the parasit-free equilibrium $E_3(1.2; 1; 0)$

is globally asymptotically stable for the interior of the first octant, so any trajectory which starts with $x(0), y(0) \neq 0$, tends to E_3 for $t \to \infty$. (see fig. 1 the red orbits)

We also depicted trajectories with $x(0) = 0$ and verified that the commensal-free equilibrium E_4 has the stable manifold $x = 0$, where as solutions with $x(0) > 0$ very small have a fast growth on the $x(t)$-component. Thus, the commensal-population, even if it is small at the begining, it multiplies in time.

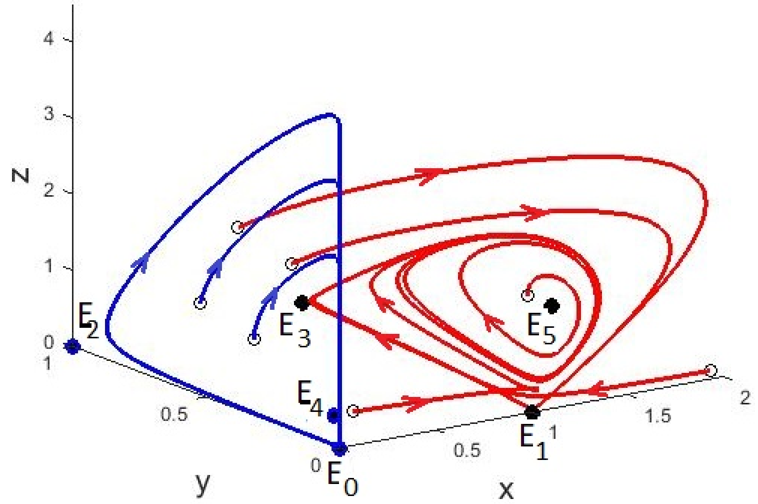

Figure 2. Two limit cycles, one of them (the ω-limit of the blue trajectories) with $W^s = \{x = 0\}$, the other one is globally asymptotically stable for the interior of the first octant. The fixed parameters are the same, $\beta_2 = 1.1 > \beta_2^H$.

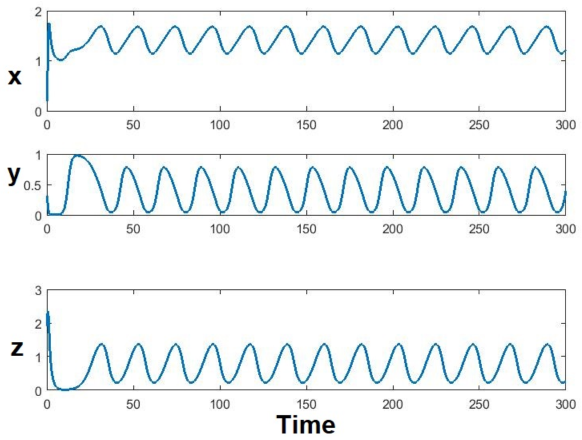

Figure 3. The time evolution of one of the solutions from the previous phase portrait, which approaches the interior limit cycle for $t \to \infty$. The initial conditions are $(0.2; 0.52; 2.098)$.

For $\beta_2 > \beta_2^H$, for example $\beta_2 = 1.1$, we depicted trajectories (see figure 2-the blue ones) which start with $x(0) = 0$ and tend to a limit cycle (see remark 3.1 for the Hopf bifurcation from the equilibrium E_4). We have $\beta_2 > \beta_2^1$. Numerical simulations showed that the stable manifold for this limit cycle is the plane $x = 0$.

Also, any trajectory which begins with $x(0) \neq 0$ very small or greater than 1 and $y(0) \neq 0$, it comes in the vicinity of the saddle connection $E_1 \to E_3$ and tends to a stable limit cycle. (theorem 3.2 with $s = 1.077 > 0$) One orbit initiated in a neighborhood of the interior equilibrium $E_5(1.4421; 0.2404; 0.8619)$ spirals towards the limit cycle, so E_5 is unstable. For a wide range of initial conditions, it appears that this limit cycle is globally asymptotically stable for the interior of $\mathbb{R}_+^3$.

For $\beta_2 \in (\beta_2^2, \beta_2^H)$, for instance $\beta_2 = 0.9$, there is a unique interior equilibrium $E_5(1.478; 0.727; 0.751)$ and it verifies the condition for local stability (theorem 2.3). Numerical simulations for a wide range of initial conditions suggests that E_5 is globaly asymptotically stable for $(\mathbb{R}_+^*)^3$. In consequance, (E_5, β_2^H) is a point of supercritical Hopf bifurcation, because when β_2 varies and passes the critical value, from a stable equilibrium E_5 for $\beta_2 < \beta_2^H$, a unique and stable limit cycle appears for each $\beta_2 > \beta_2^H$, while E_5 losses its stability.

Furthermore, the fixed parameters are $a = 0.6; b = 0.6; c = 0.6; d = 0.1; \mu = 0.2; \theta = 0.4; \beta_1 = 0.04; r = 0.8$. It verifies $d > d_0 = 0.0114$.

For $\beta_2 > \beta_2^2 = 0.8662$, we are in the conditions of theorem 3.1. We solve numerically the system (11) and we find two values for the control parameter where a saddle-node bifurcation takes place, $\beta_2^3 = 3.7119$ and $\beta_2^4 = 3.736$, so the values

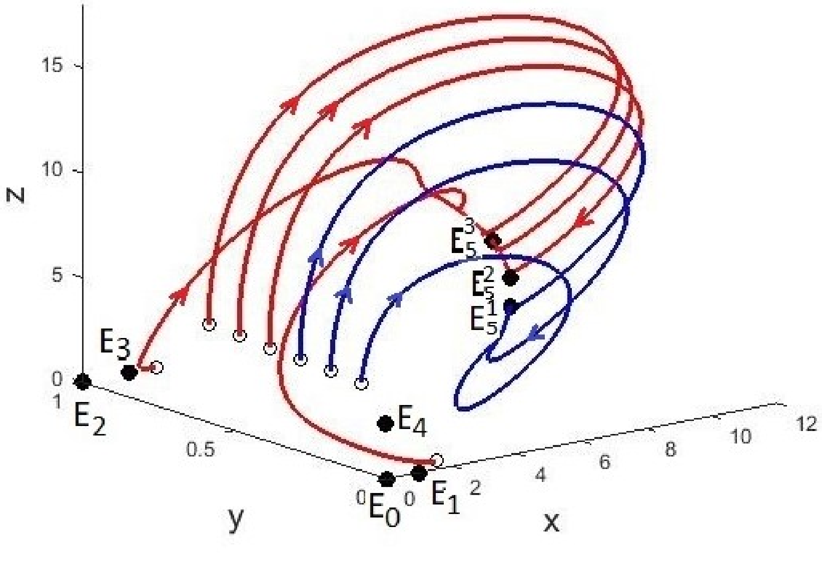

Figure 4. The phase portrait when $a = 0.6; b = 0.6; c = 0.6; d = 0.1; \mu = 0.2; \theta = 0.4; \beta_1 = 0.04; r = 0.8$ and $\beta_2 = 3.72 \in (\beta_2^3, \beta_2^4)$. There are three interior equilibria $E_5^1(5.4727; 0.1795; 5.7333)$, $E_5^2(6.1484; 0.2507; 6.5698)$, $E_5^3(6.8945; 0.388; 7.4665)$. The blue trajectories tend to E_5^1 for $t \to \infty$, the red ones to E_5^3. One trajectory comes close to E_5^2 and then tends to E_5^3.

of β_2 from proposition 2.2 which ensures the existence of three interior equilibria ($E_5^i, i = \overline{1,3}$) are the interval (β_2^3, β_2^4). For all other values of β_2, there exists a unique E_5. Numerical explorations for different sets of fixed parameters showed that $\{\beta_2 | \beta_2 = h(y), h'(y) > 0\}$ is one interval.

We took $\beta_2 = 3.72 \in (\beta_2^3, \beta_2^4)$. In the phase space, we performed simulations and we found that this a situation of bistability, namely E_5^1 and E_5^3 are asymptotically stable and the only attractors for the interior of the first octant. (see fig. 4) Indeed, only these equilibria verify theorem 2.3 of stability.

The blue trajectories tend to E_5^1 for $t \to \infty$, the red ones to E_5^3.

For the same fixed parameters, plot of the projection of the bifurcation diagram into the plane (β_2, y) for $\beta_2 > \beta_2^2$ is showen in fig. 5.

The branch of the equilibrium E_5^2 is from A to B. While β_2 crosses for example the value β_2^3 from right to left, the branches E_5^1 and E_5^2 collide, forming at $\beta_2 = \beta_2^3$ an equilibrium with $\lambda = 0$ and then dissapear. The solid and broken lines correspond to the stable and unstable equilibria. The interval (β_2^3, β_2^4) is an interval of bistability.

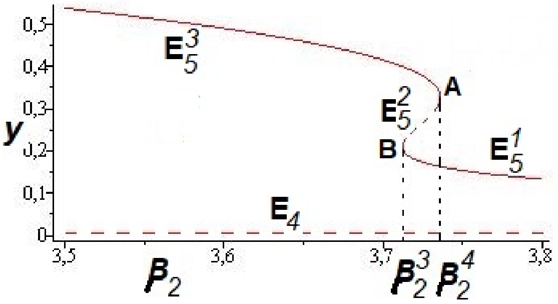

FIGURE 5. Plot of the projection of the bifurcation diagram into the plane (β_2, y) for $\beta_2 > \beta_2^2$. $a = 0.6; b = 0.6; c = 0.6; d = 0.1$; $\mu = 0.2; \theta = 0.4; \beta_1 = 0.04; r = 0.8$. The curve $\beta_2 = h(y)$ represents the interior equilibria. $(\beta_2^3, y) = (3.7119, 0.2087)$ and $(\beta_2^4, y) = (3.736, 0.3279)$ are saddle-node bifurcation points.

5. **Conclusions**

Our analysis of the model, the study of local bifurcations of codimension 1 under the variation of one parameter and the numerical simulations, lead us to establish the important types of dynamics. The control parameter that we take is β_2, the maximum growth rate of the parasite.

If $\beta_2 \in (\beta_2^0, \max(\beta_2^1, \beta_2^2))$ and $d > d_0$ (i.e. the half saturation rate d of the parasite is not too low), then for any initial conditions with $x(0) \neq 0$ (i.e. there exists initially a commensal population even very small) and $y(0) \neq 0$, the system evolves to the parasite-free state E_3 for $t \to \infty$. Notice that when the system tends to this state, $x(t) \to x_3$ and $x_3 > 1$, meaning that the commensal population advances to a number greater than its environmental carrying capacity k_1 in the absence of y and z-populations. Also, $y(t) \to 1$ for $t \to \infty$, i.e. the host population tends to its carrying capacity k_2. Our analysis revealed that the system with initial populations not zero can't evoluate to the extinction of any population, other than the parasite's.

If $\beta_2 > \beta_2^2$, in the conditions of theorem 2.3 and proposition 2.2, the system tends to an interior equilibrium E_5 and all the populations coexist in a stable state, namely $x(t) \to x_5$ for $t \to \infty$ and x_5 is greater than its environmental carrying capacity k_1, while $y(t) \to y_5$ and y_5 is less than k_2.

If we are in the hypothesis of proposition 2.2, for $\beta_2 \in (\beta_2^3, \beta_2^4)$, interval found in the numerical simulations, solutions may converge to one interior equilibrium E_5^1 or to the interior equilibrium E_5^3, depending on the initial population levels, so there are two possible states of coexistence.

We detected numerically a point of Hopf bifurcation, more precisely for $\beta_2 > \beta_2^H$ and near this value β_2^H (theorem 3.2), a stable limit cycle appears, so the populations of the system will start to oscillate, evolving in time to a periodic solution which is also a stable state of coexistence. Investigation of codimension 2 bifurcations can improve the study of all possible dynamics of the system.

REFERENCES

[1] *H. Deng, X. Huang*, The influence of partial closure for the populations to a harvesting Lotka-Volterra commensalism model, Commun. Math. Biol. Neurosci., Art. ID**10**(2018).

[2] *G.K. Edessa, B. Kumsa, P. R. Koya*, Modeling and Simulation Study of the Population Dynamics of Commensal-Host-Parasite System, American Journal of Applied Math., **6(3)**(2018), p.97-108.

[3] *R. Han, F. Chen et al.*, Global stability of a commensal symbiosis model with feedback controls, , Commun. Math. Biol. Neurosci., Art. ID (2015).

[4] *Y. A. Kuznetsov*, Elements of Applied Bifurcation Theory, Springer Verlag, New York, (1995).

[5] *Dan Littman, Eric Pamer*, Role of commensal microbiota in normal and pathogenic host immune responses, Cell Host and Microbe, **10**(2011), Iss 4, p.311-323.

[6] *J. D. Murray*, Mathematical Biology, Springer Verlag Berlin, 1989.

[7] *A. H. Nayfeh, B. Balachandran*, Applied Nonlinear Dynamics, Analytical, Computational and Experimental Methods, Wiley Series, (1995).

[8] *L.A. Reynolds, K. A. Smith et al.*, Commensal-pathogen interactions in the intestinal tract, Gut Microbes, **5**(2014), Iss 4.

[9] *C.R. Townsend, M. Begon, J.D. Harper*, Ecology: Individuals, Populations and Communities, Blackwell Science, Oxf., (2002).

[10] *P.J. Turnbaugh, R.E. Ley et al.*, The human microbiome project: exploring the microbial part of ourselves in a changing world, Nature 449,804, (2007).

[11] *R.X. Wu, L. Li et al.*, A Holling type commensal symbiosis model involving Allee effect, Commun. Math. Biol. Neurosci., Art. ID **6**(2018).